PROGRESS IN PHOTOVOLTAICS: RESEARCH AND APPLICATIONS
Prog. Photovolt: Res. Appl. 2008; **16**:649–668
Published online 6 October 2008 in Wiley InterScience (www.interscience.wiley.com) DOI: 10.1002/pip.858

Research

Coupling PV and CAES Power Plants to Transform Intermittent PV Electricity into a Dispatchable Electricity Source

James Mason[1*,†], Vasilis Fthenakis[2], Ken Zweibel[3], Tom Hansen[4] and Thomas Nikolakakis[5]
[1]*Renewable Energy Research Institute, 52 Columbia Street, Farmingdale, NY 17735, USA*
[2]*Center for Life Cycle Analysis, Columbia University, and Director of PV EH&S Research Center, Brookhaven National Laboratory, Upton, NY 11973, USA*
[3]*Institute for the Analysis of Solar Energy, George Washington University, 2121 I St. NW, Washington, DC 20052, USA*
[4]*Tucson Electric Power, P.O. Box 711, Tucson, AZ 85702, USA*
[5]*Center for Life Cycle Analysis, Columbia University, 2960 Broadway, New York City, NY 10027, USA*

This study investigates the transformation of photovoltaic (PV) electricity production from an intermittent into a dispatchable source of electricity by coupling PV plants to compressed air energy storage (CAES) gas turbine power plants. Based on historical solar irradiation data for the United States' south western states and actual PV and CAES performance data, we show that the large-scale adoption of coupled PV–CAES power plants will likely enable peak electricity generation in 2020 at costs equal to or lower than those from natural gas power plants with or without carbon capture and storage systems. Our findings also suggest that given the societal value of reducing carbon dioxide and the sensitivity of conventional generation to rising fossil fuel prices, this competitive crossover point may occur much sooner. Copyright © 2008 John Wiley & Sons, Ltd.

KEY WORDS: photovoltaics; CAES; solar energy

Received 1 February 2008; Revised 31 July 2008

INTRODUCTION

Since 1978, compressed air energy storage (CAES) plants have been in service to store excess off-peak electricity in the form of compressed air for use during peak load times. The original idea for CAES power plants was to utilize inexpensive, off-peak electricity to pressurize air at CAES plants, and to store the compressed air in underground reservoirs.[1] The stored compressed air can then be released on demand to the CAES plant's turbo-generator set to generate premium value electricity. The first CAES plant was built in Huntorf (Germany) in 1978.

The conceptualization of CAES was broadened in the 1990s as a means of solving the intermittency of wind turbine electricity production. Beginning with Cavallo,[2] numerous studies have explored the economic feasibility of coupling wind farms and CAES gas turbine (GT) power plants for base load electricity production.[3–8] The basic idea of these studies is to locate underground storage facilities in relative proximity to the wind farms and to use the CAES plants to firm and shape the intermittency of wind electricity production.

* Correspondence to: James Mason, Renewable Energy Research Institute, 52 Columbia Street, Farmingdale, NY 17735, USA.
†E-mail: je_mason@verizon.net

The wind studies demonstrate that areas of the country with high wind regimes are highly correlated with potential aquifer air storage reservoirs, which enable the location of CAES plants in close proximity to wind farms to alleviate transmission bottlenecks and the need for transmission system additions and upgrades.[8] The electricity from both wind farms and CAES plants are gathered for distribution to local markets via high voltage direct current (HVDC) power lines. The ability to locate CAES plants in close proximity to wind farms facilitates the bundling of wind and CAES electricity for long-distance transmission via HVDC power lines, which increases the capacity utilization factor of the HVDC lines from 35% for wind only electricity to 90% for wind plus CAES electricity and lowers transmission cost.

This study extends CAES research by investigating the application of CAES to resolve the intermittency of photovoltaic (PV) electricity production. We conceptualize CAES as a means of storing PV electricity that is produced in the high solar insolation areas of the Southwest US. The idea is to transport PV electricity from the Southwest to local markets throughout the US via HVDC power lines. A CAES plant is located in close proximity to the DC–AC converter station at the connection point to the local AC electricity distribution system. A portion of the PV electricity is sent to the CAES plant and stored in the form of compressed air. The CAES plant utilizes the stored compressed air to generate electricity on demand to transform the intermittent PV electricity into dispatchable peak and base load electricity for the local market.

The CAES plant serves three basic functions. For one, the CAES plant firms and shapes the portion of PV electricity consigned to grid distribution. Secondly, the CAES plant maintains a desired level of controlled electricity production capacity over the scheduled electricity production period. And thirdly, the CAES plant provides firm capacity value to a very large potential source of PV electrical energy in the US.

Our modeling of coupled PV CAES plants differs from coupled wind CAES systems in that PV plants are not necessarily located in close proximity to CAES plants. PV plants are located in the high insolation Southwest US, which has an average insolation of $6{\cdot}4\,\mathrm{kWh\,m^{-2}\,day^{-1}}$. This Southwest average insolation level translates into a 26·7% average annual capacity factor for PV power plants. The low annual capacity factor of PV power plants results in a low capacity utilization factor for the dedicated HVDC power lines, which increases transmission costs and the number of power transmission lines.[1]

There are two basic reasons for not modeling PV plants in close proximity to CAES plants. For one, water is scarce in the arid Southwest, and CAES GT power plants require substantial amounts of cooling water. And the second is the limited availability of air storage reservoirs in the suitable regions of the Southwest US, which implies that at high PV penetration levels there will not be the ability to locate CAES plants in close proximity to PV plants.

We model PV–CAES plants for both peak and base load operations. Peak PV–CAES plants are designed to produce 110 MW of power, $10\text{-h}\,\mathrm{d^{-1}}$, Monday–Friday, throughout the year. Base load PV–CAES plants are designed to produce 400 MW of power, $24\text{-h}\,\mathrm{d^{-1}}$, throughout the year, with a 90% annual availability. Our simulations are based on actual performance parameters of current PV and CAES systems and forecasts of near-term costs.[9–11]

The study evaluates levelized cost of electricity (LCOE), fuel consumption, and carbon dioxide (CO_2) emissions. The findings for PV–CAES plants are compared to conventional GT plants, natural gas combined-cycle (NGCC) plants, and coal integrated gasification combined-cycle (IGCC) plants. The NGCC and coal IGCC plants are modeled with carbon capture and storage (CCS) systems to enable the comparison of low CO_2 emissions PV–CAES power plants to low CO_2 emissions fossil fuel power plants.

The research is important because it addresses the concern of electric utilities that increasing amounts of time variant PV electricity generation connected to the nation's electrical grid could in time adversely impact reliability. Another reason this study is important is that it investigates a means of decreasing natural gas consumption for electricity production, which reduces both CO_2 emissions and demand for limited US natural gas reserves. The research is timely because of recent decreases in PV cost from the advent of second-generation, thin film PV.

[1]It should be noted that we do not model tracking systems for PV plants, which would increase the average annual capacity factor to approximately 40% with two-axis trackers, and that we do not model an HVDC system that integrates the flow of Southwest PV electricity production with the flow of Southwest or Midwest wind electricity production, which may be another means of increasing the HVDC transmission capacity utilization factor. Both of these issues are important, but due to data constraints are beyond the scope of this analysis. This study is the first in hopefully an emerging body of studies that will investigate a variety of models for PV electricity production in the Southwest US.

DOI: 10.1002/pip

The study is organized as follows. The following section develops an electricity production profile for PV power plants located in the Southwest US. The third section describes CAES power plants. Following this is a section on peak PV–CAES plants, which includes a comparison to peak fossil fuel plants. The fifth section presents the base load PV–CAES model with a comparison to fossil fuel plants with CCS systems. The final section summarizes findings.

ELECTRICITY PRODUCTION BY PV POWER PLANTS LOCATED IN THE SOUTHWEST US

The first task is to establish an electricity production profile for central PV power plants located in the Southwest US. Electricity production by PV power plants is estimated by applying the historical insolation records from the National Solar Radiation Data Base (NSRDB).[12,13] The NSRDB contains a 45-year, 1961–2005, record of insolation measurements. The NSRDB insolation records used in this study are for six locations distributed across the Southwest US—Phoenix, Tucson, Albuquerque, El Paso, Las Vegas, and Daggett.

Insolation records for the six selected sites are averaged to create a daily Southwest insolation estimate for each of the 45 years. This generates a 45-year record of average daily insolation in the geographically suitable areas of the Southwest. The insolation record provides us with information to model the effect of both intra- and inter-annual variation in insolation on PV electricity production levels.

It is assumed that PV plants are composed of flat-plate PV modules facing south and tilted at an angle equal to the site's latitude. A combination of daily and monthly NSRDB global insolation records are employed to estimate PV electricity production due to NSRDB data reporting constraints. The daily NSRDB insolation records, which are measured in hourly increments, contain data for global insolation striking a horizontal surface; these are converted to insolation on latitude-tilted surfaces.[14] The conversion of daily global insolation on horizontal surfaces to daily global insolation on latitude-tilted surfaces is based on the extrapolation of daily insolation adjustment factors generated from the measurement of changes in the monthly insolation records for latitude-tilted surfaces.

The components of PV power plants are PV modules and balance of plant components, which include land, site preparation, PV mounting supports, grounding system, wiring, transformers, and construction. PV plants producing DC electricity for grid distribution are assumed to have 85% system efficiency[15] and 99% availability.[16] We also account for 0·5% *per annum* losses due to PV module soiling and degradation, and we model the addition of PV arrays each year as part of the standard PV plant operating and maintenance schedule to compensate the soiling and degradation losses. In other words, we maintain a constant PV production level despite PV electricity losses due to annual soiling and PV module degradation.

PV cost and performance parameters are presented in Table I. PV power plant capital cost estimates are presented for 2007, 2015, and 2020 to take into account the projected development of thin film PV. The capital costs for PV power plants utilizing lowest cost PV components were \$4200 kW^{-1} in 2007.[17] In 2008, Southern California Edison announced it was contracting for thin film PV at \$3500 kW^{-1} for rooftop installations and for the California Market Referent price of 12 ¢ kWh^{-1}, after solar incentives, for a large, ground-mounted system.[18] We estimate future PV power plant capital costs of \$2000 kW^{-1} in 2015 and \$1300 kW^{-1} in 2020. The projected PV cost reductions are expected through a combination of technical advances and the realization of optimized scale economies in material flows in both PV manufacturing and installation.[19,20]

The PV technology employed for this study is cadmium telluride (CdTe) thin film PV patterned after First Solar's module product,[21] which at present is the lowest cost PV module technology.[2] Since CdTe thin film PV is a new technology, its technological progress is rapid. Also, increases in the manufacturing scale of PV modules will further reduce PV module costs. The balance of plant costs and operating expenses for PV power plants are based on the German Juwi Group 40 MW plant and the Tucson Electric Power Springerville 4·6 MW PV plant.[10,17] As with PV module costs, balance of plant costs are expected to decline

[2]Ongoing PV research suggests the potential for other PV technologies such as crystalline silicon (c-Si), amorphous silicon (a-Si), copper–indium–gallium–selenium (CIGS), and gallium arsenide concentrator PV technologies to match the projected 2020 cost of electricity estimates for CdTe thin film PV. Our projections are based on CdTe thin film PV because its development history provides relatively high confidence in future cost and performance projections.

DOI: 10.1002/pip

Table I. PV–CAES and GT peak power plant cost and performance assumptions*

(Constant 2007 $ US)	2007	2015	2020	Reference
Capital costs				
PV modules ($\$\,kW^{-1}$)	2 200	1 000	650	40
PV balance of plant ($\$\,kW^{-1}$)	1 800	1 000	650	40
CAES turbo-generator set ($\$\,kW^{-1}$)	190	190	190	37
CAES compressor ($\$\,kW^{-1}$)†	175	175	175	37
CAES peak balance of plant ($\$\,kW^{-1}$)	230	230	230	33
CAES-base load balance of plant ($\$\,kW^{-1}$)*	139	139	139	33
CAES peak compressor/turbine power ratio	1·09	1·09	1·09	
CAES-base load compressor/turbine power ratio	2·21	2·21	2·21	
CAES air storage reservoir ($\$\,kWh^{-1}$)*	2·00	2·00	2·00	
NG GT plant ($\$\,kW^{-1}$)	485	485	485	11
HVDC overhead lines ($\$\,km^{-1}$)	485 000	485 000	485 000	22
HVDC converter station (million $/station)	475	475	475	22
Performance assumptions and costs				
PV plant system efficiency	0·85	0·85	0·85	15
PV plant operational availability	0·99	0·99	0·99	40
PV O&M ($ per year)	750 000	750 000	750 000	40
PV plant annual capacity factor	26·7%	26·7%	26·7%	40
Average Southwest insolation ($kWh\,m^{-2}\,day^{-1}$)	6·4	6·4	6·4	13
Transmission losses (per 2400 km)	0·06	0·06	0·06	22
HVDC DC–AC conversion efficiency (%)	0·99	0·99	0·99	22
Power connection to compressors (%)‡	0·97	0·97	0·97	
CAES plant energy ratio (kWh_{in}/kWh_{out})	0·84	0·84	0·84	
CAES peak plant heat rate ($MJ\,kWh^{-1}$)	5·064	5·064	5·064	
CAES-base load plant heat rate ($MJ\,kWh^{-1}$)	4·819	4·819	4·819	
CAES plant fixed O&M ($\$\,kW^{-1}$)	3·69	3·69	3·69	11
CAES plant variable O&M ($\$\,kWh^{-1}$)	0·006	0·006	0·006	11
CAES parasitic power loss (% of output)	2%	2%	2%	
NG GT heat rate ($MJ\,kWh^{-1}$)	12·24	12·24	12·24	11
NG GT fixed O&M ($\$\,kW^{-1}$)	20·3	20·3	20·3	11
NG GT variable O&M ($\$\,kWh^{-1}$)	0·0043	0·0043	0·0043	11
NG GT parasitic power loss (% of output)	2%	2%	2%	

Notes:
*All dollar amounts are presented in constant 2007 $. If the reference is blank, then the data entry is original to this study. Heat rates are reported at the fuel's high heat value.
†The compressor cost estimate is the baseline cost stated in terms of $\$\,kW^{-1}$ of turbine power output and needs to be scaled by the compressor/turbine power ratio to establish the actual compressor cost for the peak and base load CAES plants.
‡We assume 3% electricity losses at the compressor station due to low electricity flow levels that are not sufficient to meet the compressors minimum power requirements. This electricity loss rate is not based empirical data but is included as a conservative loss factor.

with increased module output per unit area, i.e., increases in PV efficiency, scale economies in the manufacture and purchase of balance of plant components, and technical progress.

On a final note, a national electricity transmission system is required to transport the large quantities of PV electricity from remote Southwest locations to local markets throughout the US. Therefore, an HVDC transmission system is included as an integral component of the PV electricity production and distribution system. We project a 6% electricity loss for the average 2400 km transmission distance between PV plants and distributed CAES plants over the HVDC transmission network.[22] An additional 1% electricity loss is modeled for the conversion of DC to AC electricity at the DC–AC converter stations.[22] We model three DC-AC converter stations per 2400 km of the HVDC transmission system. The estimated levelized cost of HVDC electricity transmission is $\$0{\cdot}024\,kWh^{-1}$ and is derived from the HVDC cost and performance parameters in Table I, the financial parameters in Table II, and a 26·7% HVDC capacity

DOI: 10.1002/pip

Table II. Financial assumptions to estimate cost of electricity*

Construction period†	Three years
Capital payments: three equal payments	Three equal payments
Ratio of equity capital to debt capital	45% Equity/55% debt
Nominal return on equity	10·0% Per Year
Nominal return on debt	6·5% Per Year
Real capital charge rate (weighted average cost of capital)	5·0%
Annual inflation rate	1·9%
Property tax and insurance (CAES plant)	2% Of initial capital per year
Property tax and insurance (PV plant)‡	1% Of initial capital per year
Working capital	15% Of annual change in expenses
Depreciation	MACRS
Corporate tax rate	38·20%
Replacement cost (occurring in years 10 and 20)	5% Of initial capital
30-Year book life; 20-year tax life	

Notes:
*The LCOE estimates are calculated by the net present value cash flow method.[41]
†PV installation is incremental, which means that revenues can be generated during the construction period. The three-year construction period is for construction of the CAES GT plant and the air storage reservoir.
‡Insurance rate is assumed to be 0·5% of initial capital since insurance is required only for PV modules. Property tax is assumed to be 0·5% of initial capital since PV plants are located in the largely unpopulated Southwest US.

utilization factor for the distribution of PV electricity from the Southwest.[3]

The development of an HVDC electricity transmission system out of the Southwest and spanning the US will require national level planning and implementation. At present, it is very difficult to gain right-of-ways for long-distance power lines. Assuming a 5–7 gigawatt (GW) capacity for HVDC power lines,[23,24] approximately 200 HVDC power lines will be required to transport a terawatt of PV power capacity. While the development of a HVDC transmission system to support super large-scale Southwest PV electricity production will present challenges, it is doable.[24,25]

The sizing of HVDC power lines has to accommodate the peak electricity production of PV's power capacity, which occurs for only a brief period each day. The inherent daily profile of PV electricity production means that dedicated HVDC lines are underutilized. To address concerns over the low capacity utilization of a costly HVDC system, an abbreviated analysis of an alternative system composed of distributed PV–CAES plants, where the PV and CAES plants are built in close proximity to one another throughout the country, is performed to assess the economic efficacy of the Southwest PV and distributed CAES model.

[3]If only one DC–AC converter station is required for the 2400 km HVDC line, then the levelized cost of electricity transmission is $0.016 kWh with a 26.7% capacity utilization factor.

Another possibility that we did not model is to simply build distributed PV fields linked to peak natural gas plants to shape and firm the PV electricity. However, this would be similar to the use of standby reserve capacity of natural gas plants, which results in more fuel consumption and CO_2 emissions than PV–CAES plants. Other HVDC combinations could also be studied, e.g., PV–CAES with higher capacity factor from tracking PV; PV combined with wind, which can be quite complementary and allows for much higher capacity factors than either alone. On a final note, intercontinental HVDC is also possible with the potential to raise capacity use to over 50% for solar alone, but such long lines have very high expenses and many other challenges.

CAES POWER PLANTS

CAES GT power plants are similar to conventional GT power plants with the key exception that air compressors are separated from the turbo-generator set. The turbo-generator set consists of a high- and low-pressure expander-turbine units and electricity generators. In conventional GT plants, a single shaft connects the compressors and turbo-generator train, and the energy to compress air consumes approximately two-thirds of the energy generated by the turbine. In the CAES plant design, the separation of compressors from the turbo-generator set enables all of

DOI: 10.1002/pip

the turbine's mechanical energy to be used for electricity generation, which triples the turbine's electricity generation capacity.

CAES power plants use an external source of electricity to provide the energy for air compression. The compressed air is then stored in underground reservoirs. The stored compressed air is released on demand to provide kinetic energy to power the plant's turbines. Suitable underground storage reservoirs are salt formations, aquifers, and depleted gas fields. It has been demonstrated that approximately 75% of the US land area have geological formations suitable for underground storage of compressed air for CAES plants.[26] Underground compressed air storage reservoirs are assumed to be able to deliver 95% of the stored working air capacity. Management of reservoir gas deliverability rates is a normal annual operating and maintenance task.[27]

Two commercial CAES power plants are currently operating—the 290 MW Huntorf, Germany plant commissioned in 1978 and the 110 MW McIntosh, Alabama plant commissioned in 1991. Both plants are peak electricity production plants and have proved reliable. A 110 MW CAES power plant is employed as a peak power plant in this study, which enables the application of performance parameters reported for the McIntosh, Alabama 110 MW CAES plant. The base load plant in this study is a 400 MW CAES plant. The performance parameters of the base load CAES plant are scaled in proportion to performance parameters of the 110 MW CAES plant.[4]

The primary components of a CAES power plant are the turbo-generator set, compressors, an air storage reservoir, a heat exchange recuperator that captures the exhaust heat from the turbine and uses it to preheat air flowing from the storage reservoir, and balance of plant components that include, which include a water cooling system for the compressors, an air piping system to and from the storage reservoir, air drying and purification units for air injected and withdrawn from the air storage reservoir, and plant construction.

A CAES plant requires an airflow rate of 5·05 kg kWh^{-1} with an inlet air pressure of 4341 kPa to the high-pressure expander-turbine unit.[28] The air storage reservoir must be sized to have a working air capacity sufficient to maintain a minimum reservoir air pressure of 4534 kPa to sustain the required airflow rate to the expander-turbine unit. Working air capacity is the quantity of air in the storage reservoir that is above the minimum pressure of 4534 kPa. The quantity of air that always remains in the storage reservoir to maintain the minimum reservoir pressure is referred to as base or cushion gas.

Air is compressed to a pressure of 7584 kPa for storage. We estimate energy consumption for air compression with an adiabatic compression energy formula

$$W_{J\cdot kg^{-1}} = (y/y-1)P_1V_1\left[(P_2/P_1)^{(y-1)/y}-1\right] \times [(Z_1+Z_2)/(2Z_1)]/\text{Efficiency} \quad (1)$$

where $W_{J\cdot kg^{-1}}$ = specific compression work; y = specific heat ratio (adiabatic coefficient); P_1 = initial pressure (PaA); P_2 = final pressure (PaA); V_1 = initial specific volume (m^3 kg^{-1}); Z_1 = gas compressibility factor for initial pressure; Z_2 = gas compressibility factor for final pressure; and efficiency = efficiency of the compressors.[29] The gas compressibility factor is estimated by the Redlich–Kwon Equation of State method.[30] A compressor efficiency of 80% is assumed over the 0·1–7·6 MPa range of pressures.

The energy to compress air from 0·1 MPa to 7·6 MPa is estimated to be 0·522 MJ kg^{-1} of air. It follows that the energy ratio of a CAES plant, which is the ratio of electricity input for compression to the electrical energy output by the turbo-generator set, is 0·73 kWh$_{in}$/kWh$_{out}$ with four-stage compression.[5] The energy ratio is less than unity due the fact that electrical energy input is supplemented by the thermal energy of natural gas burnt in the combustors.

The quantity of fuel consumed by the McIntosh CAES plant is 55% less than the fuel consumed by a single-cycle GT plant per kWh of electricity output.[11] Reduction or even elimination of the need of fuel is pursued in advanced adiabatic CAES (AA–CAES) concepts that capture, store, and utilize compression heat; these could be commercialized by 2015–2020.[31,32] Even if AA–CAES does not succeed in completely eliminating the need of fuel, it is certain that the operation of CAES plants would require even

[4]The proportional scaling assumption is to simplify the presentation and is not expected to hold in all instances. For example, in a study of 150 and 350 MW CAES plants the airflow rate for the 350 MW plant is 9% less than the airflow rate of the 150 MW plant on a MW rated basis[33]. The implication of this difference on the conclusions of our study is that we are over-stating the air storage capacity for base load CAES plants by approximately 5%, which is within an acceptable margin of error for this type of general study.

[5]From our literature review, reported energy ratios range from 0·67 to 0·81[28,8] (ERPRI, 2003).

DOI: 10.1002/pip

less fuel in the future, and instead of natural gas, biofuels or hydrogen could be used. Conservatively, our current modeling is solely based on the fuel consumption of the McIntosh plant.

Our capital cost estimate for air storage reservoirs at CAES plants is $2·00 kWh^{-1} of working air storage capacity.[6] Air storage reservoir cost estimates are derived from an Electric Power Research Institute (EPRI) study and apply to saline aquifers, depleted natural gas wells, and excavated salt domes.[33]

CAES plant air storage capacity is a function of daily air injection/withdrawal balances. For PV–CAES plants, the daily air injection rate is contingent on PV electricity production, and the daily withdrawal rate is contingent on CAES plant size and the daily electricity production schedule. These are calculated as follows:

$$\text{Air storage balance} = \sum (\text{Air } i\text{njection/day} - \text{Air withdrawal/day}) \quad (2)$$

and

$$\text{Air injection/day (kg)} = \frac{(W_{\mathrm{p}}\, I_{\mathrm{ph}} Eff)(1 - TL)}{C_e} \quad (3)$$

where W_{p} = PV capacity and the subscript p indicates power output at peak insolation, which is defined as 1000 W m^{-2}, I_{hp} = hours of peak insolation per day ((Wh d^{-1})/1000 W), Eff = PV power plant system efficiency (85%), TL = electricity transmission losses between the PV plant and CAES plant compressor station (7%) plus a 3% allowance for electricity losses at the low ends of PV electricity transmission, i.e., PV electricity production is too low to enable compressor operation, C_e = energy to compress air for underground storage at 7584 kPa (166 Wh kg^{-1}); and

$$\text{Air withdrawal/day (kg)} = \frac{T_e \text{h/d}}{\text{AF/MWh}} \quad (4)$$

where T_{e} = CAES power plant capacity and the subscript e indicates nameplate power rating, h/d = hours of plant operation per day, AF/MWh = airflow rate kg/MWh (5047 kg MWh^{-1}).

A cost optimization algorithm is used to determine PV capacity and air storage reservoir volume for the peak and base load PV–CAES models.[7] The optimization algorithm minimizes the aggregate cost for PV capacity and the air storage reservoir. For a given working air capacity, the optimum PV capacity is the minimum for which the cavern does not deplete for more than 0·5% of the total 45-year record of solar radiation measurements. The process is repeated for a wide range of working air capacities, and for each working air capacity the optimum PV capacity and total cost are determined. The end result is a PV capacity and a working air storage volume that corresponds to a minimum cost.

There will be times during the year, primarily from mid-spring through mid-fall when the air injection rate will exceed the air withdrawal rate and result in periods where air storage capacity is at its maximum. During these periods, the PV electricity dedicated to air compression at the CAES plants is not needed. It is assumed that this excess PV electricity will be routed onto the electricity transmission grid for general distribution. The routing of excess PV electricity to the grid is possible since DC–AC converter stations are an integral component of the HVDC transmission system to the CAES plant, which uses AC electricity to power the compressors.

CAES power plant technology is well suited to transform intermittent PV electricity into a source of dispatchable electricity. CAES plants are able to ramp-up and ramp-down power output to accommodate daily PV electricity production while also supporting variable utility loads if needed. The ramp rate of CAES plants is ±27% of maximum power capacity per minute.[28]

PEAK PV–CAES POWER PLANTS

A schematic of the daily electricity production profile of a coupled peak PV–CAES plant is presented in

[6]The air storage cost metric, $ kWh^{-1}, is calculated by dividing total air storage cost by the total quantity of electricity that can be produced with one complete air injection/withdrawal cycle for a given working air storage capacity.

[7]The operational formula for the optimization algorithm is: min (x) where: x = an array containing components x_i (i = 1,2,3 …); x_i = 0·18 (mil $/mil lb of air)*C$_i$ + 1.3 (mil $/MW of installed PV)*P$_i$; C$_i$ = cavern working capacity (mil lbs); C$_i$ = i(mil lbs); P$_i$ = PV plant optimum capacity (MW) corresponding to C$_i$. Subject to: P$_i$ = min (P), for which Tod ≤(0.5% × td) where: P: an array containing components P$_j$ and j = 1,2,3…i...; P$_j$ = pv to grid + j (MW); pvtogrid = the portion of total PV capacity sending electricity directly to the grid (MW); Tod = total days the cavern depletes over the 45 year period; and td = total days constituting the 45 years period (16 425 days).

DOI: 10.1002/pip

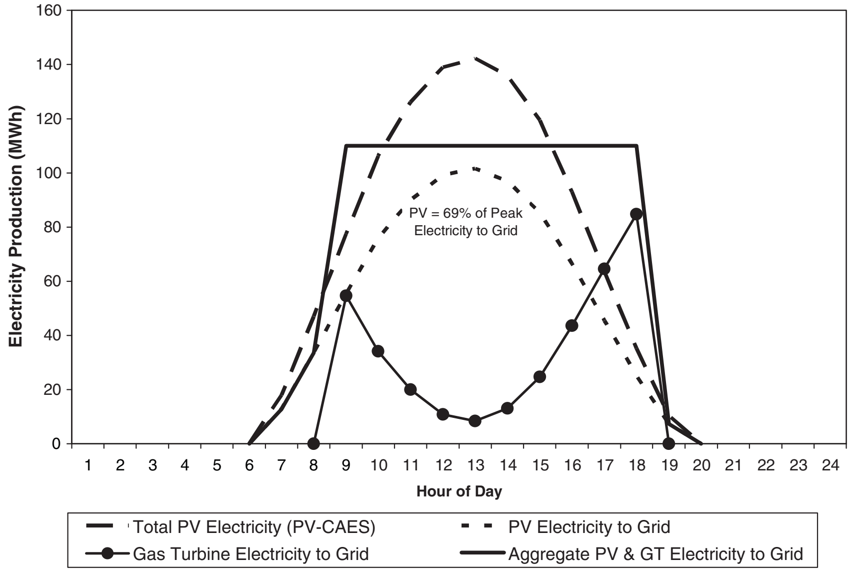

Figure 1. Graphic depiction of peak period electricity production by a coupled 158 MW PV plant and a 110 MW CAES plant. Notice that the PV electricity production curves represent average insolation conditions. In reality, there will be fluctuations in PV electricity production, and the power production of the CAES GT plant is ramped up or down as needed to maintain a constant 110 MW level of electricity production

Figure 1. All PV electricity is transported via HVDC. The CAES plant is located in proximity to the local market that the electricity will supply, and a DC–AC converter station is built in close proximity. The DC PV electricity once converted to AC electricity is then routed to local markets and to the CAES plant. When the CAES plant's air storage reservoir is at maximum capacity, 100% of PV electricity is routed to the local market.

The objective is to couple a PV power plant to a 110 MW CAES GT power plant to insure a firm supply of 110 MW of power to meet peak load conditions, $10\,h\,d^{-1}$, Monday–Friday. Our optimization model shows that 158 MW of PV rated capacity is needed for the coupled PV and CAES plants to supply a continuous 110 MW of power under worst winter conditions. The model allows for 15% PV plant losses and 7% transmission losses. Of the total PV capacity, the electricity produced by140 MW of the PV capacity is for grid distribution, Monday–Friday, and the remaining 18 MW is for air compressions at the CAES plant, Monday–Friday. On weekends, all PV electricity is used for air compression.

While the Figure 1 graph shows a constant 10-h supply of electricity, a peak CAES power plant has the ability to vary the level of electricity production over the course of the day to match variable electricity demand. For example, in many utility territories the peak electricity demand in the summer months occurs from 5–7 PM, and in winter months there is a dual peak in electricity demand. Winter peak demand for electricity occurs in the early morning hours, 7–9 AM, and then again in the evening hours, 5–9 PM. PV–CAES plants have the ability to tailor daily electricity production to meet both summer and winter electricity demand schedules.

On average, over a year, electricity production from the 158 MW PV plant accounts for 68% of the total PV–CAES electricity sent to the transmission grid for local distribution. This level of PV electricity production reduces the average daily utilization factor for the CAES plant to 11%, which results in a large reduction in fuel consumption. The remainder of the 110 MW load is satisfied directly from PV electricity. The aggregate fuel consumption for the total grid distributed electricity produced by coupled peak PV–CAES plants is 86% less than that for the same level of electricity production by peak GT plants.

The quantity of compressed air stored by a CAES power plant needs to be sufficient to enable the power plant to meet its electricity production schedule in the presence of variable PV electricity production levels.

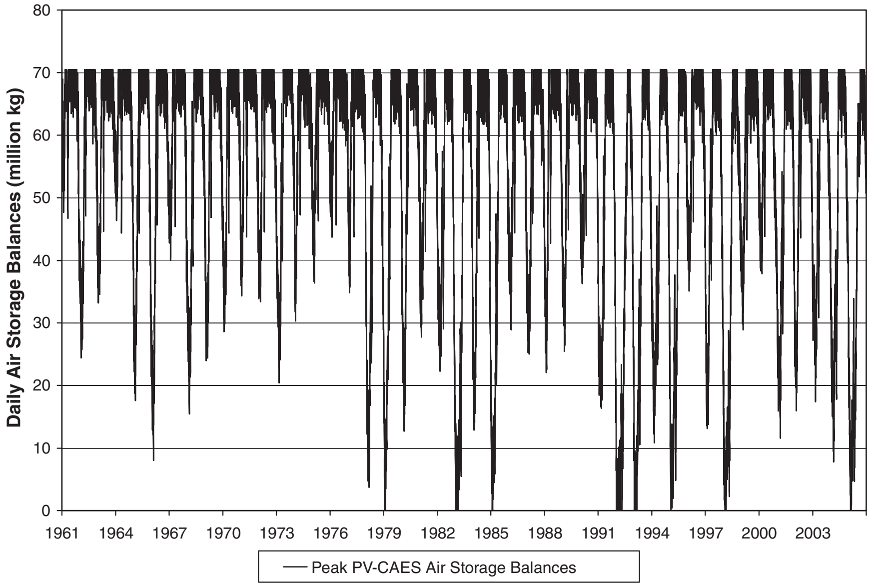

Figure 2. 45-year record of daily air storage balances for a peak 110 MW PV–CAES plant operating 10-h d^{-1}, Monday–Friday with 83 million kg of working air storage capacity

The cost optimization results indicate that the required working air storage capacity is 767 512 cubic meters at 7584 kPa and 15·6°C. This stored air capacity enables the CAES plant to operate for 127 h over one complete air injection/withdrawal cycle without any air injection.

Daily air storage injection/withdrawal balances are presented in Figure 2. As shown, there are periods when air storage is depleted. The number of days *per annum* that air storage becomes depleted is presented in Figure 3. Notice that air storage depletion only occurs in years with extreme weather conditions. In most instances, extreme weather patterns, which are expected to cause extended periods of below average insolation, can be forecasted in advance. With this knowledge, normal CAES plant operation can be altered to conserve stored air and prevent depletion of the air storage reservoir.

The lowest air injection/withdrawal balances occur in the years 1992 and 1993, which corresponds to the effects of the atmospheric ash concentration caused by the Mt. Pinatubo volcano eruption in 1991. A volcano eruption on the scale of the Mt. Pinatubo eruption has occurred only four times in the past 400 years. During this most extreme event, CAES capacity shortfalls occur for only 25 days. Since, an event like the 1991 Mt. Pinatubo eruption can be forecasted months in advance, there is ample time to bring alternate energy sources on line or to reduce the operating time of the CAES plant to avoid serious disruptions in electricity supply. Hence, the 127 h of stored working air capacity is sufficient for continuous operation of the peak CAES plant under all but the most extreme adverse climate conditions.

Using LCOE estimation methods common in the power generation industry, the LCOE for aggregate electricity production by coupled peak PV–CAES plants are \$0·269 kWh^{-1} in 2010, \$0·166 kWh^{-1} in

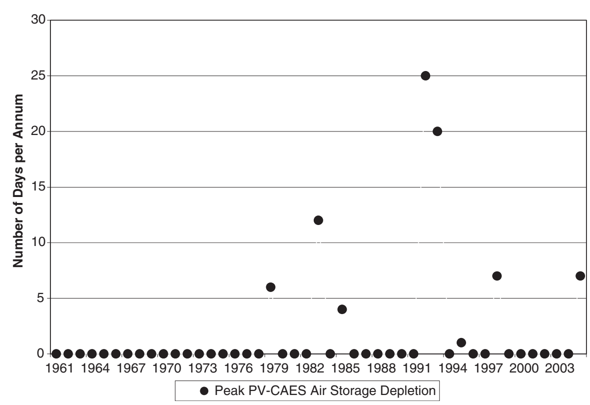

Figure 3. Number of days per year that the air storage reservoir becomes depleted for a peak PV CAES plant with the assigned PV and working air storage capacities

DOI: 10.1002/pip

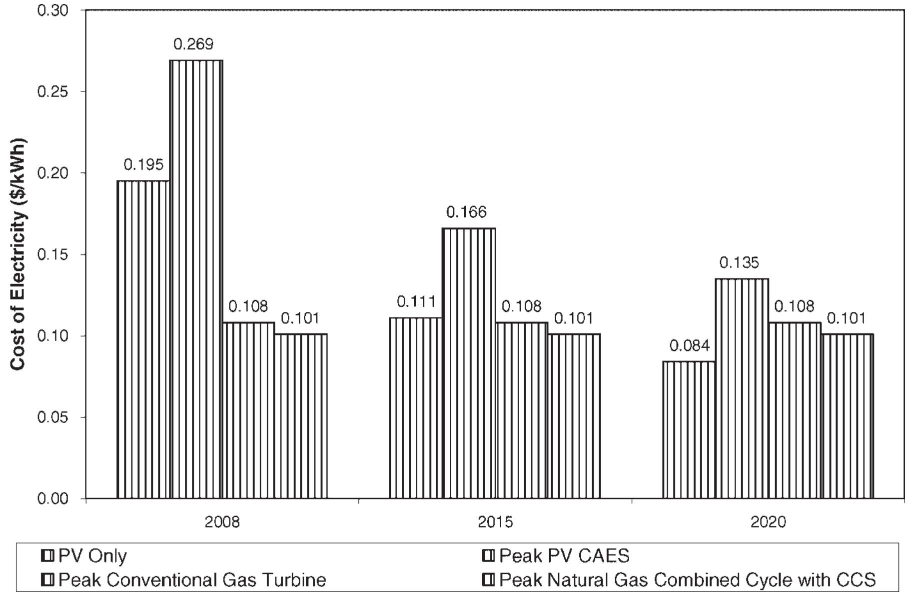

Figure 4. Cost of electricity comparison between PV only, peak PV CAES plants, peak conventional GT plants, and peak NGCC plants with CCS. The assumed fuel price for natural gas is \$6 GJ^{-1}, which is the approximate contract natural gas price for electric utilities in the US in 2006, which is the last year for reported information. However, contract natural gas price for electric generating companies has risen above \$6 GJ^{-1}, which means that the fuel price sensitivity findings presented in Figure 6 are the best means to compare cost of electricity

2015, and \$0·135 kWh^{-1} in 2020 (refer to Figure 4). The assumed fuel price is \$6·0/GJ for natural gas.[8] An HVDC transmission cost of \$0·024 kWh^{-1} is included in the PV–CAES cost of electricity estimates. An average transmission between PV and CAES plants of 2400 km is assumed with 7% electricity losses, which includes the 1% loss incurred at the DC–AC converter station. The CO_2 emissions rate for PV–CAES plants is 97 g $CO_2\,kWh^{-1}$, which includes the contributions from the combustion of natural gas and from the life-cycle of CO_2 emissions for the PV electricity[35,36].

The electricity cost estimates presented in this study are derived through the net present value cash flow method with the financial assumptions presented in Table II. The financial assumptions are based on EPRI–DOE[37] with downward insurance and property tax adjustments for PV power plants located in the remote Southwest US.[9] We are not attempting to derive definitive cost of electricity estimates since estimates are sensitive to variation in financial assumptions. On a final note, financial incentives such as investment tax credits and the effects of potential carbon taxes are not included in the cost of electricity estimates.

Sensitivity analyses are performed to evaluate the effect of changes in fuel cost, PV and CAES plant capital costs, and HVDC transmission distance on PV–CAES cost of electricity. The effect of fuel cost on PV–CAES cost of electricity is presented in Figure 6. A \$1/GJ change in fuel cost changes the cost of electricity by \$0·0015 kWh^{-1}. The small sensitivity of cost of electricity to changes in fuel cost is attributable to the small amount of natural gas consumed by coupled PV–CAES power plants. The sensitivity of the cost of electricity to changes in the other factors is presented in Figure 7. A \$100 kW^{-1} change in PV and CAES plant capital costs changes the cost of electricity by \$0·004 and \$0·003 kWh^{-1}, respectively, and a change in HVDC transmission distance of 500 km changes the cost of electricity by \$0·005 kWh^{-1}.

We now turn our attention to a comparison of cost of electricity for 2020 peak PV–CAES plants to those for conventional peak GT power plants and NGCC power plants. The cost of electricity comparison is presented

[8]The natural gas price of \$6 GJ^{-1} is lower than the average 2007 and 2008 contract natural gas price for US electricity generators.
[9]The Southwest US land area suitable for PV plants is undeveloped, hence low property taxes. Also, approximately 50% of the costs for PV plant components do not qualify for insurance since they have zero risk for loss, for example mounting supports, underground conduit, land, etc.[34]

DOI: 10.1002/pip

in Figure 4. The cost of electricity estimate is \$0·108 kWh^{-1} for conventional peak GT plants and \$0·101 kWh^{-1} for peak NGCC plants. Notice in Figure 6 the greater sensitivity of GT and NGCC cost of electricity to changes in fuel cost due to the greater fuel consumption rate of peak GT and NGCC plants compared to peak PV–CAES plants. While the comparative cost of electricity findings indicate that at relatively low natural gas prices peak GT and NGCC power plants produce lower cost electricity than peak PV–CAES plants, the recent upward trend in natural gas prices suggests that by 2020 peak PV–CAES plants may become a cost competitive source of peak electricity supply without any economic recognition of the value of their carbon dioxide reduction.

The CO_2 emissions rate for conventional GT plants is 553 g CO_2 kWh^{-1},[35] which is seven times greater than the aggregate CO_2 emissions rate for PV–CAES peak plants. Comparative power plant CO_2 emissions rates are presented in Figure 5. The installation of CCS systems at peak GT plants results in a significant increase in the cost of electricity and because of this has not been included in the analysis. On the other hand, NGCC plants with CCS systems produce low cost electricity and produce less CO_2 emissions than does a coupled PV–CAES plant. There is no indication that peak electricity production by coal power plants with CCS systems is cost competitive since the costs of coal power plants are much greater than GT plants, and coal steam turbine plants do not have fast ramp-up and ramp-down capabilities.

The capital cost of a 2020 peak PV–CAES plant is \$2749 kW^{-1}, which is a factor of 5·7 greater than the \$485 kW^{-1} capital cost of a conventional peak GT plant and a factor of 2·3 greater than the \$1172 kW^{-1} capital cost of a peak NGCC plant with CCS. However, annual fuel and O&M expenses are greater for peak GT and NGCC plants compared to peak PV–CAES plants. Notice in Figure 6 that when fuel cost exceeds \$8·5/GJ that the cost of electricity for peak PV–CAES plants is lower than that for peak GT plants and when fuel cost exceeds \$10·2/GJ that the cost of electricity for peak PV–CAES plants is lower than that for peak NGCC plants with CCS.

Even the 2015 PV–CAES numbers can compare favorably with conventional generators if the price of fuel reaches the high end of the sensitivity domain given in Figure 6. The effect of high fuel cost on annualized cash flows can offset the capital cost differential between peak PV–CAES power plants and peak GT and NGCC with CCS power plants. Since the course of fuel prices is largely unpredictable, it is possible that PV–CAES may become cost-competitive well prior to 2020. Another factor that is not accounted in our comparison are the safety risks related to transportation and storage of CO2, a heavier than air asphyxiant gas.[38]

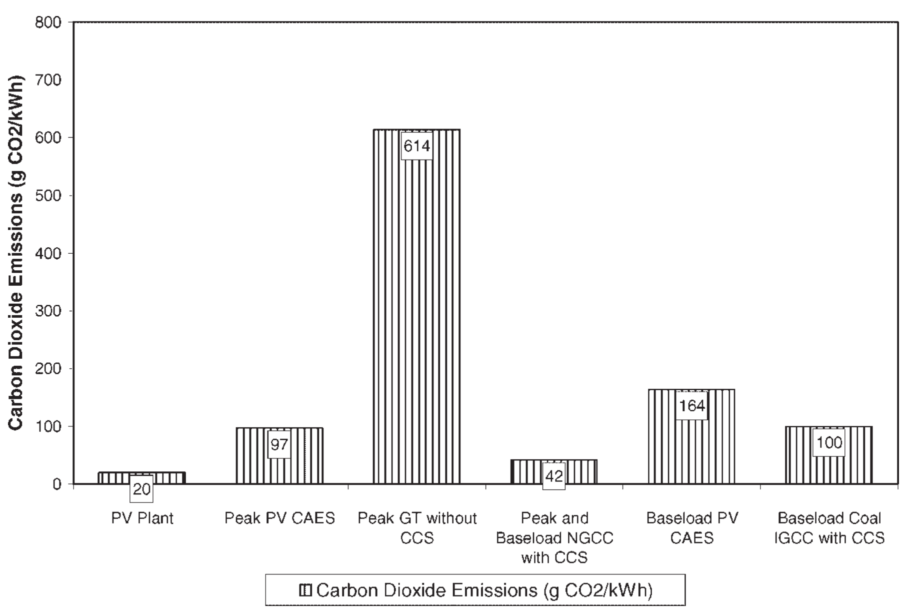

Figure 5. Power plant carbon dioxide emissions per kilowatt-hour of electricity produced

DOI: 10.1002/pip

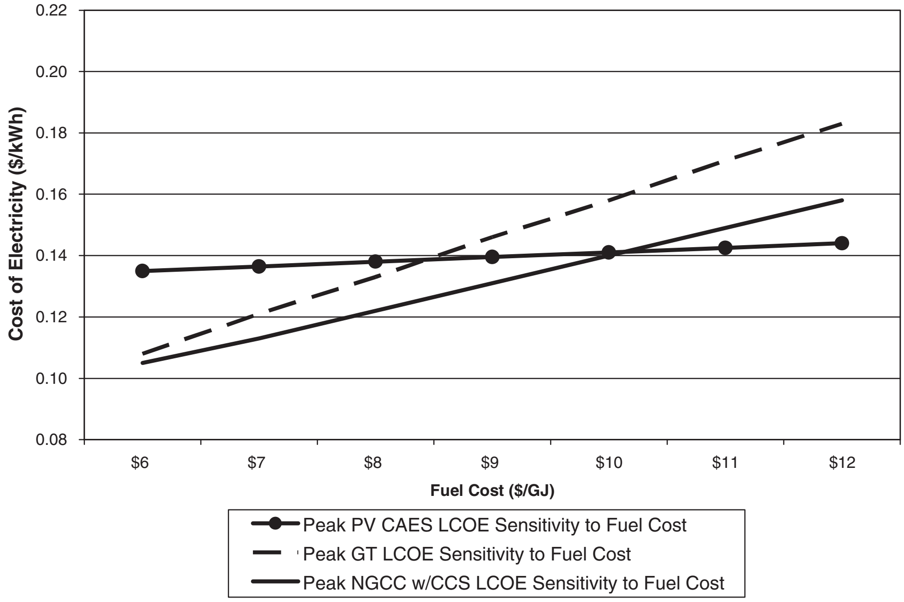

Figure 6. Sensitivity of peak PV–CAES, conventional GT, and NGCC power plants LCOE to changes in fuel cost. The modeled power plants operate on average 10 h day^{-1}, Monday–Friday, which is a 30% capacity factor

The final issue to be considered in the analysis of peak PV–CAES plants is the economic justification of HVDC distribution of Southwest PV electricity to CAES plants distributed outside the Southwest. As noted in the sensitivity findings, the impact of HVDC cost on peak PV–CAES cost of electricity is approximately \$0·005 kWh^{-1} per 500 km of transmission distance. The impact of reduced insolation on

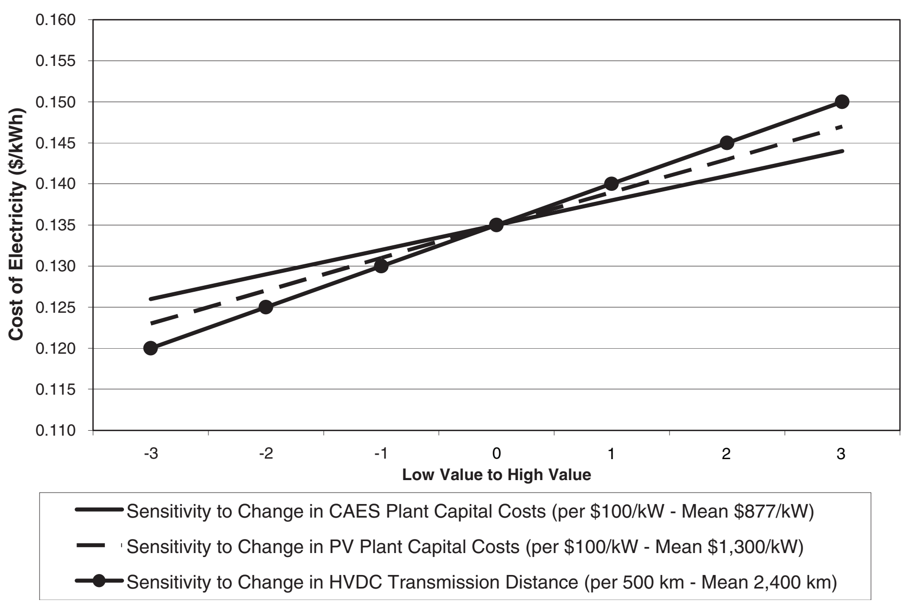

Figure 7. Sensitivity of peak PV–CAES LCOE to changes in CAES plant capital costs, PV plant costs, and to HVDC transmission distance

DOI: 10.1002/pip

the cost of electricity from distributed PV–CAES plants is presented in Figure 8. A 0·5 kWh m^{-2} day^{-1} reduction in average insolation increases the cost of electricity from distributed PV–CAES plants by \$0·006 kWh^{-1}.

The insolation level corresponding to the breakeven cost for transporting or not transporting electricity from the Southwest via HVDC power lines occurs at locations with an insolation level of 5·2 kWh m^{-2} day^{-1}. This insolation level occurs at locations surrounding the Southwest. It should be noted that, after accounting for the cost of transmission, the cost of electricity from the Southwest to locations in the North/Northeast US with insolation of 3·4 kWh m^{-2} day^{-1}, is only 15% higher than the cost of local PV electricity generation. This finding suggests that distributed PV–CAES plants may be an economical option throughout the US.

Although we focus on the long-term issue of storing and using solar energy at high penetration levels, we recognize that until that time, various lower cost schemes for using PV electricity will be adopted. For example, charging CAES with wind and then using that energy to smooth real-time solar output is a practical, lower cost approach of making low-carbon dioxide, low-cost energy than PV–CAES. And using wind and solar together is a better way to increase the capacity utilization of HVDC. Finally, until there is a mandate to build an extensive national HVDC network, distributed PV with traditional fossil backup will likely be the most prevalent way PV is used.

BASE LOAD PV–CAES POWER PLANTS (POST-2020)

In contrast to peak PV–CAES plants, it is assumed that base load PV–CAES plants are not built until post-2020 when PV costs are reduced to the minimum projected levels. However, this could change if fossil fuel prices continue to soar or if non-CO_2 alternatives are unavailable. The electricity production schedule for base load plants is 400 MW of power, 24 h day^{-1}, year round, minus plant maintenance downtime. The annual availability of base load PV–CAES plants is assumed to be 90%.

The cost of electricity for base load PV–CAES plants is compared to the cost of electricity for base load NGCC plants and coal IGCC plants and both outfitted for CCS. The financial assumptions for cost of electricity estimates are presented in Table II. Capital cost and performance parameters for base load NGCC and coal IGCC plants are presented in Table III. Fuel costs for cost of electricity estimation are assumed to be \$6/GJ for natural gas and \$1·8/GJ for coal.

CCS system costs include power plant CO_2 capture, pipeline transport of CO_2 to storage reservoirs,

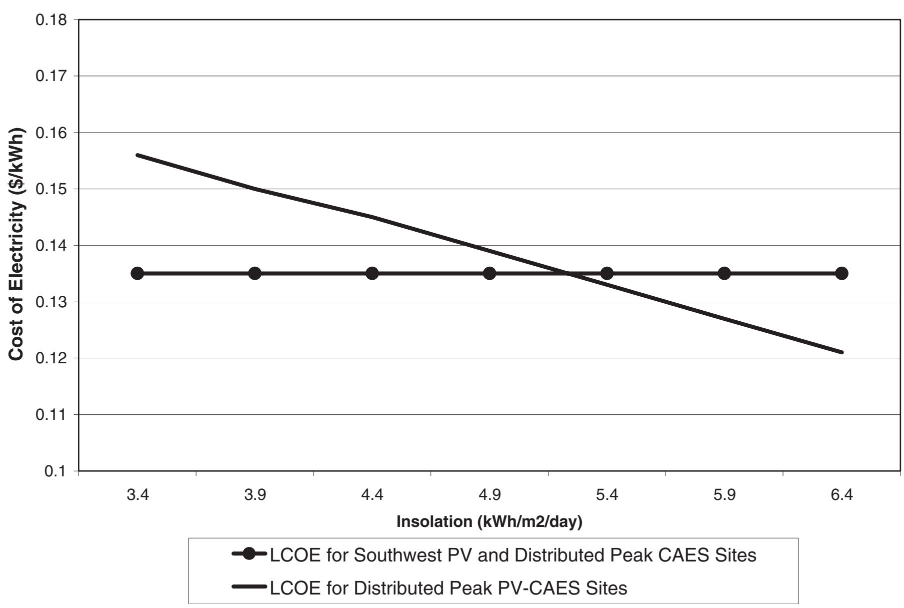

Figure 8. LCOE comparison of distributed peak PV CAES plants to Southwest PV plants coupled to distributed peak CAES plants

DOI: 10.1002/pip

Table III. Fossil fuel power plant cost and performance parameters[39]*

A. Natural gas CC with CCS		
Total plant costs ($\$\,kW^{-1}$)	1172	39
Plant capacity factor	0·85	39
Fixed O&M ($\$\,kW^{-1}$)	16·637	39
Variable O&M ($\$\,kWh^{-1}$)	0·0026	39
Heat rate ($MJ\,kWh^{-1}$)	8·237	39
Parasitic power loss (% Of power output)	7%	39
GHG emissions (g $CO_2\,kWh^{-1}$)	42	39
B. Coal IGCC with CCS		
Total plant costs ($\$\,kW^{-1}$)	2496	39
Plant capacity factor	0·8	39
Fixed O&M ($\$\,kW^{-1}$)	44·586	39
Variable O&M ($\$\,kWh^{-1}$)	0·0082	39
Heat rate ($MJ\,kWh^{-1}$)	11·227	39
Parasitic power loss (% of Power output)	25%	39
GHG emissions (g $CO_2\,kWh^{-1}$)	100	39

*Heat rates are reported at the high heat value.

reservoir development, and long-term reservoir monitoring. Cost estimates for CO_2 transport, storage, and monitoring are reported to be \$0·004 kWh^{-1}.[39] However, these estimates are based on very optimistic conditions, a CO_2 transport distance of only 80 km and compressors at only the point of CO_2 production, and therefore may not be representative of true CO_2 transport costs. The results of a sensitivity analysis indicate that the cost of electricity sensitivity to a \$100 kW^{-1} change in CCS costs is \$0·001 kWh^{-1} for NGCC and coal IGCC power plants.

For base load PV–CAES plants, the PV electricity production profile created from the 45-year NSRDB insolation record indicates that a 1·613 GW PV power plant will support a 400 MW base load CAES power plant. The electricity output from 507 MW of the total PV capacity is dedicated to grid distribution, and the electricity output from the remaining 1106 MW of PV capacity is consigned to the CAES plant for air compression. This allocation of PV electricity occurs 7 days a week, year-round.

The volume of the air storage reservoir for the base load CAES plant is 6·88 million cubic meters of working air capacity at 7584 kPa and 15·6°C. This quantity of stored compressed air is able to maintain 312 h of CAES plant operation without any air injection. Daily air storage balances are presented in Figure 9, and the number of days *per annum* that air storage is depleted is presented in Figure 10. Just as in the peak PV–CAES scenario, the time of year with lowest air storage balances is the low insolation late-fall and winter months. Hence, plant maintenance downtime should be scheduled in late-fall and early winter to recharge and conserve air storage capacity. On the other hand, compressor maintenance downtime should be scheduled in the high insolation spring period when reservoir recharging is relatively rapid. Also, notice in Figure 10 that the years when air storage depletion occurs are those years experiencing extreme low insolation climate conditions such as the years following the 1991 Mt. Pinatubo volcano eruption with the maximum air storage depletion of 29 days. As stated previously, these low insolation climate conditions can be forecast in advance and CAES plant operating schedule adjusted to conserve air storage capacity.

With the base load PV–CAES model adopted for this study, PV plants directly produce 36% of aggregate PV–CAES electricity production, and the CAES plant produces the remaining 64%. The average daily CAES operating factor is 72%. In 2020, the aggregate cost of electricity estimate for base load PV–CAES plants is \$0·118 kWh^{-1}. The PV–CAES cost of electricity estimate includes \$0·024 kWh^{-1} to transport electricity via HVDC power lines from the Southwest PV plants to distributed CAES plants at an average distance of 2400 km and with 7% electricity losses. The aggregate CO_2 emissions rate is 164 g $CO_2\,kWh^{-1}$, which includes the CAES plant contribution from the combustion of natural gas and the life-cycle CO_2 emissions for PV electricity.[35,36]

The capital costs for a 400 MW-base load CAES plant with a supporting 1·613 GW PV plant are

DOI: 10.1002/pip

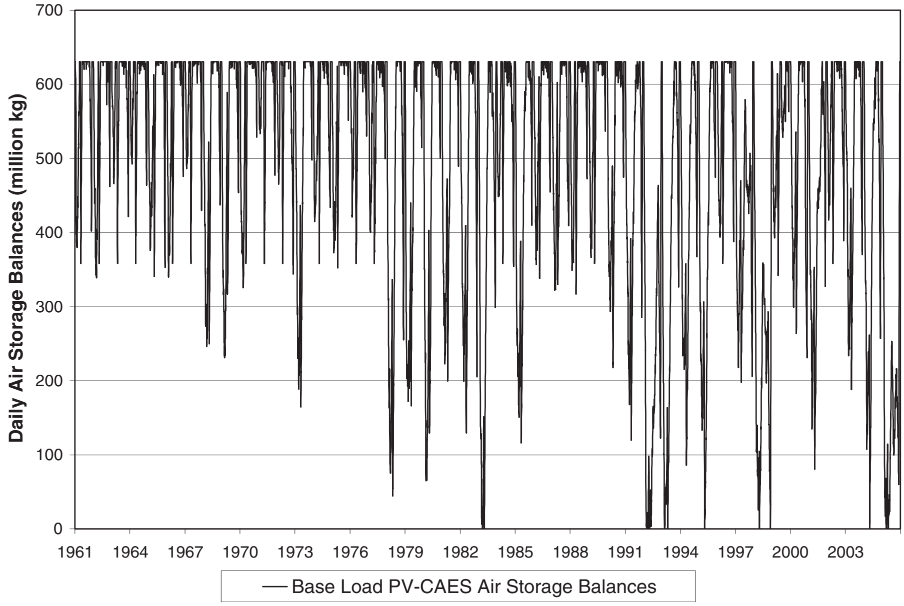

Figure 9. 45-year record of daily air storage balances for a base load PV–CAES plant. The operating schedule includes 36 days of turbo-generator set downtime for normal maintenance scheduled from December 1 to January 6 each year, and 10 days of compressor downtown for normal maintenance scheduled from April 21–April 30 each year

$6681 kW^{-1}. In contrast, the capital costs for 400 MW NGCC and coal IGCC plants with CCS are $1172 and $2496 kW^{-1}, respectively.[39] The cost of electricity estimate for base load PV–CAES plants is $0·118 kWh^{-1}. The base load PV–CAES cost of electricity estimate is compared to the cost of electricity estimates for the base load NGCC and coal IGCC plants, and the findings are presented in

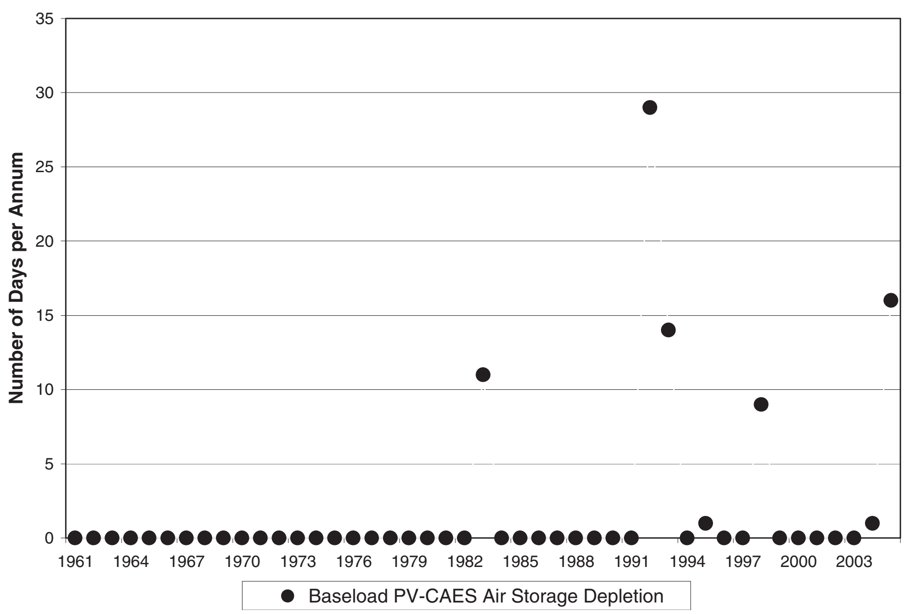

Figure 10. Number of days per year that the air storage reservoir becomes depleted for a base load PV CAES plant with the assigned PV and working air storage capacities

DOI: 10.1002/pip

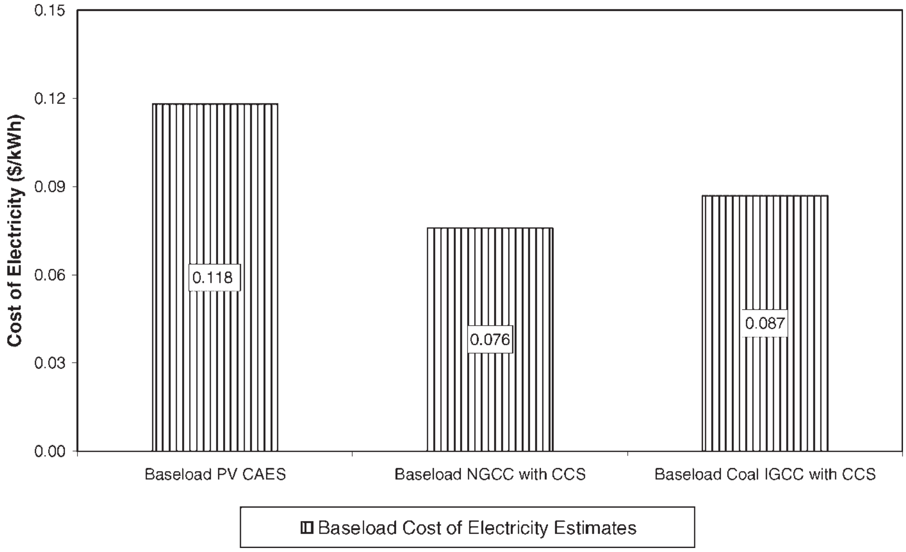

Figure 11. Cost of electricity estimates for base load PV–CAES (2020 PV model) and base load Natural Gas CC and Coal IGCC power plants with CCS. Assumed fuel prices: natural gas = \$6 GJ^{-1}; coal = \$1·8 GJ^{-1}

Figure 11. The reported electricity cost estimate for base load NGCC plants is \$0·076 kWh^{-1}, and the estimate for base load coal IGCC plants is \$0·087 kWh^{-1}, which are 36% and 26% lower than the cost of electricity for base load PV–CAES plants, respectively.

The sensitivity of cost of electricity for the base load power plants to change in fuel cost is presented in Figure 12. As expected, the cost of electricity from NGCC plants is the most sensitive to change in fuel cost. The breakeven cost of electricity for base load PV–CAES and NGCC plants with CCS is \$0·141 kWh^{-1}

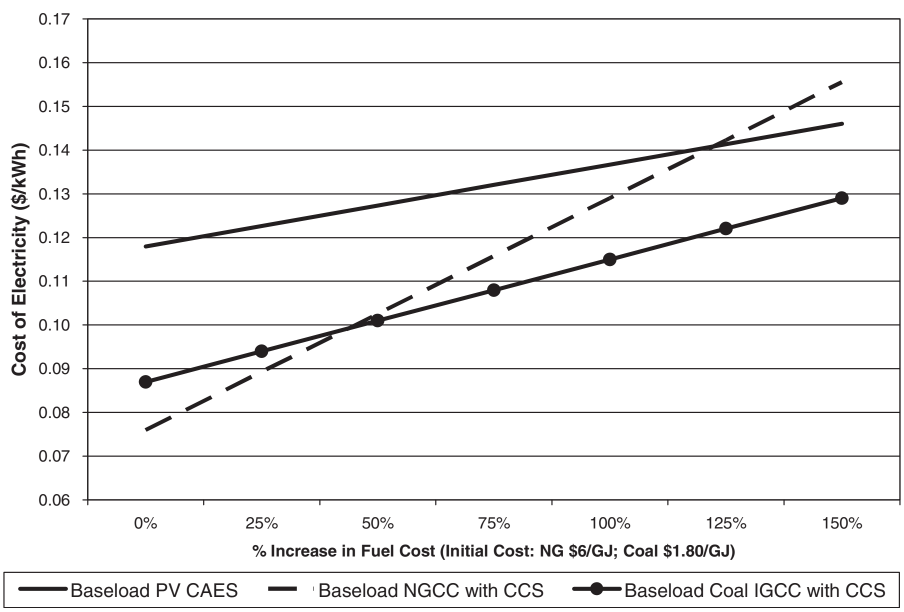

Figure 12. Sensitivity of cost of electricity to increases in fuel cost for base load PV–CAES plants, NGCC plants, and coal IGCC power plants with CCS

DOI: 10.1002/pip

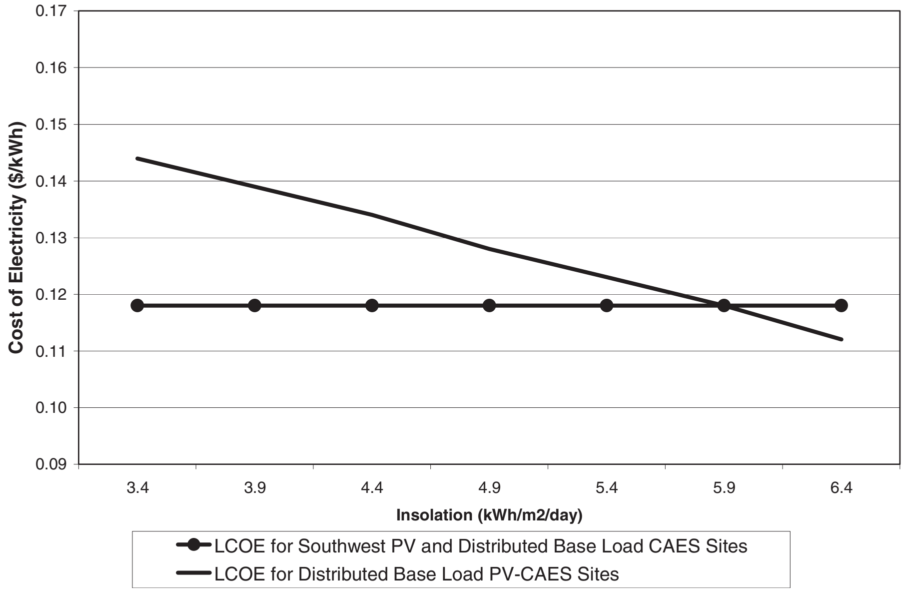

Figure 13. LCOE comparison of distributed base load PV CAES plants to Southwest PV plants coupled to distributed base load CAES plants

and occurs with a fuel cost of $\$13{\cdot}5\,\mathrm{GJ}^{-1}$, which is 125% greater than the $\$6\,\mathrm{GJ}^{-1}$ baseline fuel cost.

The determination of the breakeven cost of electricity between 2020-modeled PV–CAES and coal IGCC plants is problematic since two fuels are involved. Based on the cost of electricity trajectories for base load PV–CAES and coal IGCC plants presented in Figure 12, it is unlikely that the fuel cost mix will result in base load PV–CAES as an economically viable option in 2020. In addition, it should be noted that the base load PV–CAES cost of electricity estimates are significantly greater than the cost of electricity estimates for base load wind-CAES plants.[7,8]

As with the peak PV–CAES scenario, an analysis of distributed base load PV–CAES plants is performed, and the cost of electricity estimates compared to those for the model with PV electricity generated in the Southwest and transmitted via HVDC to CAES plants distributed across the country. The comparison is presented in Figure 13. The cost of electricity breakeven point occurs at locations with an average insolation level of $5{\cdot}9\,\mathrm{kWh\,m^{-2}\,day^{-1}}$, which is substantially greater than the peak PV–CAES finding. Locations with an average insolation level of $5{\cdot}9\,\mathrm{kWh\,m^{-2}\,day^{-1}}$ can only be found in the Southwest. But once again, the impact on cost of electricity is relatively small, 22% greater than that at worst case insolation locations, which implies that distributed base load PV–CAES plants may be an economically feasible option.

CONCLUSION

A summary of the findings for the 2020-modeled peak and base load PV–CAES plants is as follows. The aggregate LCOE for peak PV–CAES plants is $\$0{\cdot}135\,\mathrm{kWh}^{-1}$, and for base load PV–CAES plants it is $\$0{\cdot}118\,\mathrm{kWh}^{-1}$. The aggregate fuel consumption for peak PV–CAES plants is $2{\cdot}0\,\mathrm{MJ\,kWh}^{-1}$, and for base load PV–CAES plants it is $3{\cdot}55\,\mathrm{MJ\,kWh}^{-1}$. The aggregate CO_2 emissions rate for peak PV–CAES plants is $97\,\mathrm{g}\ CO_2\,\mathrm{kWh}^{-1}$, and for base load PV–CAES plants it is $164\,\mathrm{g}\ CO_2\,\mathrm{kWh}^{-1}$.

And important finding is that by 2020 peak PV–CAES plants might be cost competitive with peak electricity production by conventional GT power plants and by NGCC with carbon and capture systems power plants. On the other hand, our findings suggest that the cost of electricity for base load PV–CAES plants will not be cost competitive with other sources of base load electricity supply in 2020, unless fuel prices increase dramatically from current levels.

While the capital cost of coupled peak PV–CAES plants is a factor of two or more greater than the capital

DOI: 10.1002/pip

cost of comparable fossil fuel peak power plants, the low heat rate of peak PV–CAES plants moderates the effect of fuel costs on annualized cash flows, and significantly improves the economic viability of peak PV–CAES plants. Such effect would be even greater, if, as expected near-adiabatic CAES plants are developed by 2020.

Our peak PV–CAES findings are important since there is a relatively good chance that natural gas prices in 2020 will be at a high enough level to make peak PV–CAES electricity production cost competitive. The natural gas cost level where the cost of electricity for peak PV–CAES plants is equal to the cost of electricity for conventional peak GT plants without CCS systems is $\$8{\cdot}5\,GJ^{-1}$ and for NGCC power plants with CCS it is $\$10{\cdot}2\,GJ^{-1}$. These natural gas prices are not that much higher than the 2007 electric utility contract price for natural gas. Indeed, if natural gas prices take a continued rising path, we may have to revisit the economics of the 2015 peak PV–CAES model.

The low heat rate of peak PV–CAES plants is conducive for the utilization of bio-syngas, which if used by PV–CAES plants will result in a near-zero CO_2 emissions path. With a bio-syngas cost of $\$13\,GJ^{-1}$, the 2020 cost of electricity for a peak PV–CAES plant is $\$0{\cdot}146\,kWh^{-1}$, which is cost competitive with peak GT power plants at a natural gas cost of $\$9{\cdot}0\,GJ^{-1}$ and with NGCC plants with CCS systems at a natural gas cost of $\$10{\cdot}5\,GJ^{-1}$.

To distribute PV electricity produced in the Southwest to local markets throughout the country will require the construction of a national HVDC power distribution system. To distribute the electricity from a PV power plant capacity of one terawatt will require the construction of 200 5-GW HVDC lines. While this will require extensive planning, it is considered doable based on current planning for extensive HVDC systems in China and India. And the cost is not prohibitive since it increases the cost of electricity produced by PV–CAES plants at an average 2400 km transmission distance by only $\$0{\cdot}024\,kWh^{-1}$.

An alternative to a national HVDC system to distribute Southwest PV electricity is distributed PV plants located throughout the country and in close proximity to distributed CAES plants. While the cost of electricity by distributed PV power plants is greater than the Southwest PV model, the net increase in cost of electricity at the lowest US insolation site is just 15%. Therefore, distributed PV–CAES plants may prove economically viable. However, it should be noted that factors other than insolation may increase the cost of distributed PV–CAES plants relative to Southwest PV plants and distributed CAES plants such as a need for costly concrete mounting foundations to protect against tornado activity, high land costs, and increased fuel consumption by the CAES plant in response to greater diurnal variability in insolation. In conclusion, distributed PV–CAES plants require greater depth of analysis than provided in this study before a firm conclusion can be reached.

We do not consider numerous other possible short, mid-, and long-term combinations of PV, CAES, HVDC, wind, other renewables, and conventional backup. These deserve further study as they may represent practical paths in terms of economics and carbon dioxide avoidance.

On a final note, the operating life of PV modules is longer than 30 years and may exceed 60 years. In addition, the operating life of PV balance of plant components, i.e., PV mounting supports and underground wiring conduits, is at least 60 years in the arid environment of the Southwest. Therefore, the reduction in cost of electricity accruing from amortization of power plants would be more favorable for PV–CAES plants than aging fossil fuel plants. This means a large post-amortization decrease in electricity prices from PV–CAES plants, which translates into an economically attractive long-term electricity price trajectory for PV–CAES power plants.

REFERENCES

1. Zaugg P. Air-storage power generating plants. *Brown Boveri Review* 1975; **62**: 338–347.
2. Cavallo AJ. High-capacity factor wind energy systems. *Journal of SolarEnergy Engineering, Transactions of the ASME* 1995; **117**: 137–143.
3. Denholm P, Kulcinski GL, Holloway T. Emissions and energy efficiency assessment of baseload wind energy systems''. *Environmental Science and Technology* 2005; **39**: 1903–1911.
4. Desai N, Gonzalez S, Pemberton DJ, Rathjen TW. The Economic Impact of CAES on Wind in TX, OK, and NM. Ridge Energy Storage & Grid Services L.P., Texas State Energy Conservation Office June 27 2005.
5. Denholm P. Improving the technical, environmental and social performance of wind energy systems using biomass-based energy storage. *Renewable Energy* 2006; **31**(2006): 1355–1370.
6. Cavallo A. Controllable and affordable utility-scale electricity from intermittent wind resources and compressed air energy storage (CAES). *Energy* 2007; **32**: 120–127.

DOI: 10.1002/pip

7. Greenblatt JB, Succar S, Denkenberger DC, Williams RH, Socolow RH. Base load wind energy: modeling the competition between gas turbines and compressed air energy storage for supplemental generation. *Energy Policy* 2007; **35**: 1474–1492.
8. Succar S., Williams RH. *Compressed Air Energy Storage: Theory, Resources, and Applications for Wind Power*. Report prepared by the Energy Systems Analysis Group, Princeton Environmental Institute, Princeton University 2008.
9. Fthenakis Vasilis, James M, Mason E, Ken Zweibel. The technical, geographical and economic feasibility for solar energy to supply the energy needs of the United States. *Energy Policy, In press.*
10. Mason JE, Fthenakis VM, Hansen T, Kim HC. Energy payback and life-cycle [$_2$co] emissions of the bos in an optimized 3.5-mw pv installation. *Progress in Photovoltaics: Research and Applications* 2006; **14**(2): 179–190.
11. DeCorso Richard, Lee Davis, Dennis Horazak, John Molinda, Mario DeCorso. Parametric study of payoff in applications of air energy storage (CAES) plants – an economic model for future applications.'' Paper presented at *Power Gen International Conference*, Orlando, Florida, November 2006.
12. NREL. *National Solar Radiation Data Base, 1961–1990*. Renewable Resource Data Center, National Renewable Energy Laboratory (NREL), Golden, CO. http://rredc.nrel.gov/solar/old_data/nsrdb 2007a.
13. NREL. *National Solar Radiation Data Base, 1991–2005*. Renewable Resource Data Center, National Renewable Energy Laboratory (NREL), Golden, CO. http://rredc.nrel.gov/solar/old_data/nsrdb 2007b.
14. Marion W, Wilcox S. *Solar Radiation Data Manual for Flat-Plate and Concentrating Collectors*. Manual Produced by the National Renewable Energy Laboratory's Analytic Studies Division. Contract No. NREL/TP-463-5607, DE93018229, April 1994.
15. Falck L. Personal communication with Lars Falck of the JUWI Group 2008.
16. Hansen TN. The promise of utility scale solar photovoltaic (pv) distributed generation. Presented at POWER-GEN International, Las Vegas, NV, 10 December 2003.
17. Juwi. 2007, Press release ''World's largest solar power plant being built in eastern Germany.'' http://www.juwi.de/international/information/press/PR_Solar_Power_Plant_Brandis_2007_02_eng.pdf
18. Lesser J, Puga N. PV vs. solar thermal. Public Utilities Fortnightly July 2008: 2008, 17–20, 27.
19. Zweibel K. The terawatt challenge for thin film pv. In *Thin Film Solar Cells: Fabrication, Characterization and Applications*. Poortmans J, Archipov V (eds). Boston, John Wiley, 2005 1396–1408.
20. Keshner MS, Arya R. 2004; *Study of Potential Cost Reductions Resulting from Super-Large-Scale Manufacturing of PV Modules*. Final Subcontract Report, NREL/SR-520-36846, October (2004), National Renewable Energy Laboratory, US Department of Energy, Golden, CO. http//:www.nrel.gov/docs/fy05osti/36846.pdf
21. Ginley D, Green M, Collins R. Solar energy conversion toward 1 terawatt. *MRS Bulletin* 2008; **33**(4): 355–364.
22. DLR. *Trans-Mediterranean Interconnection for Concentrating Solar Power*. German Aerospace Center (DLR), Institute of Technical Thermodynamics, Section Systems Analysis and Technology Assessment. Federal Ministry for the Environment, Nature Conservation and Nuclear Safety, Stuttgart, Germany 2006.
23. de Andrés J., Miques Pérez, Miguel Mühlenkamp, Dietmar Retzmann, Roland Walz. Prospects for HVDC: getting more power out of the grid. Presentation prepared for Siemens AG and presented at *the CIGRE Conference*, Madrid, Spain, 29–30 November 2006.
24. Dorn Joerg, Dietmar Retzmann, Cristen Schimpf, Dag Soerangr. HVDC solutions for system interconnection and advanced grid access. Presentation for Siemens AG at *the EPRI HVDC Conference*, 13–14 September 2007.
25. McCoy Paul, Vaninetti Jerry. It's doable: building transmission for solar. *EnergyBiz* 2008; **5**(2): 40.
26. Mehta B. 1992, CAES geology. EPRI J 1992 (October/November): 38–41.
27. AGA. *Examining Natural Gas Storage for Local Distribution Companies*. Final report prepared by International Gas Consulting, Inc., Houston, TX for the American Gas Association (AGA), Washington, DC, May 1998.
28. Davis L., Schainker BR. *Compressed Air Energy Storage (CAES): Alabama Electric Cooperative McIntosh Plant – Overview and Operational History*. Report prepared jointly by the Alabama Electric Cooperative and the Electric Power Research Institute (EPRI). EPRI; Palo Alto, CA 2006.
29. Schwartz J. The gas compression formula was given to Mason by Joseph Schwartz, a gas dynamics engineering specialist with Praxair 2005.
30. Peress J. Working with non-ideal gases: here are two proven methods for predicting gas compressibility factors. *CEP Magazine* 2003; 39–41.
31. Bullough C., Gatzen C, Jakiel C, Koller M, Nowi A, Zunft S. Advanced adiabatic compressed air energy storage for the Integration of wind energy. *Presented at the Proceedings of the European Wind Energy Conference*, EWEC 2004, 22–25 November 2004, London UK.
32. Zunft S., Christoph J, Martin K, Chris B. Adiabatic compressed air energy storage for the grid integration of wind power. *Presented at the Sixth International Workshop on Large-Scale Integration of Wind Power and Transmission Networks for Offshore Windfarms*, 26–28 October 2006, Delft, The Netherlands 2006.
33. Swensen E, Potashnik B. *Evaluation of Benefits and Identification of Sites for a CAES Plant in New York*

DOI: 10.1002/pip

State. Report prepared by Energy Storage and Power Consultants in association with ANR Storage Company for Electric Power Research Institute (EPRI). TR-104288, Research Project, Final Report, August 1994, EPRI, Palo Alto, CA 1994.
34. EIA. *Annual Energy Outlook* Energy Information Administration (EIA), DOE/EIA-0554 (2007), US Department of Energy, Washington, DC, March 2007.
35. Wang M. GREET Version 1.7 (Excel Interactive Version). Center for Transportation Research, Argonne National Laboratory, University of Chicago, Chicago, IL 2001.
36. Fthenakis V, Hyung M, Chul K. Greenhouse-gas emissions from solar electric- and nuclear power: a life cycle study. *Energy Policy* 2007; **35**(4): 2540–2557.
37. EPRI-DOE. *EPRI-DOE Handbook of Energy Storage for Transmission and Distribution Applications*. Report Number 1001834, Electric Power Research Institute (EPRI), Palo Alto, CA and the US Department of Energy, Washington, DC 2003.
38. Elgin B. The dirty truth about clean coal. *Business Week June* 2008; **30**: 55–56.
39. NETL. *Cost and Performance Baseline for Fossil Energy Plants*, Vol. 1. Report DOE/NETL-2007/1281, National Energy Technology Laboratory (NETL): Washington, DC, May 2007.
40. Zweibel K, James EM, Vasilis F. A solar grand plan. *Scientific American* 2008; **298**(1): 64–73.
41. Copeland TE, Weston JF. *Financial Theory and Corporate Policy*, 3rd Ed. Addison-Wesley Publishing Company: Reading, MA, USA 1992.

DOI: 10.1002/pip